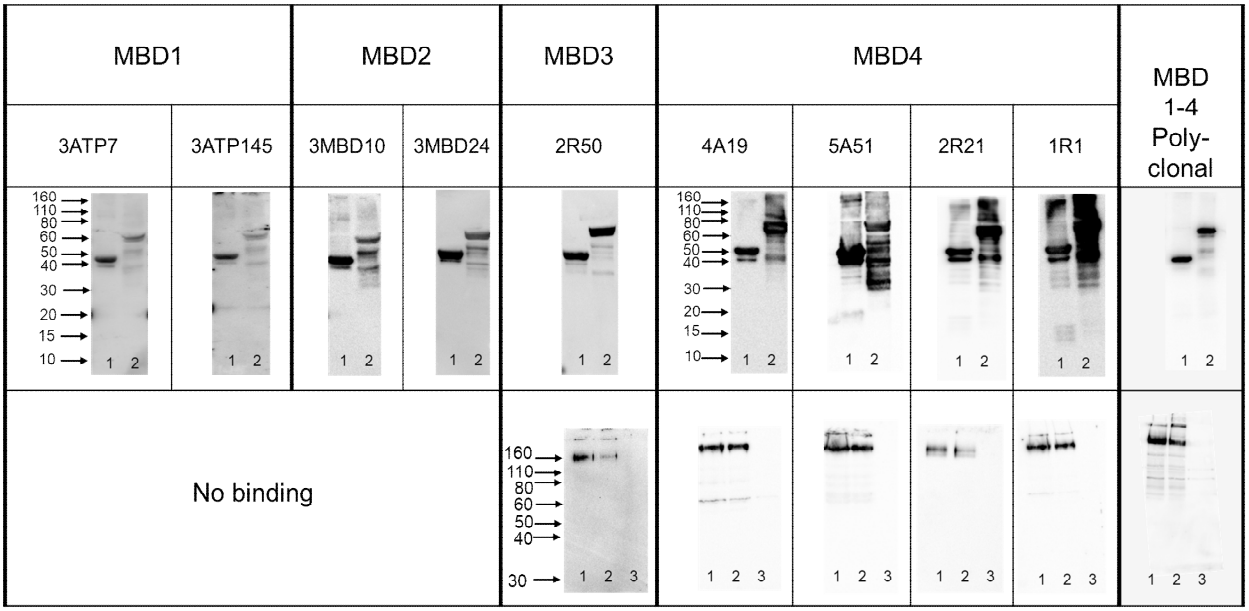

Fig. S1 Detection of the purified MBD1-4, MBD1-6 and complete ATP7B by the Nanobodies on Western blots. MBD1-4 (*upper row*, lane 1 on each blot), MBD1-6 (*upper row*, lane 2 on each blot), or membrane preparations from HEK293 cells expressing recombinant wild type ATP7B (*lower row,* lane 1 on each blot), catalytically inactive D1027A mutant variant (*lower row*, lane 2 on each blot), or endogenous ATP7B only (*lower row*, lane 3 on each blot) were probed with Nanobodies against each of the first four MBDs, as indicated in the table header. Positions of molecular weight markers (KDa) are shown on the left for each group of blots. The blots were incubated with the Nanobodies, as primary antibodies, at a concentration of 0.6 μg/ml for the Nanobodies against MBD3 and MBD4, when probing MBD1-4 and MBD1-6 blots, and 6 μg/ml for all other blots. Western blots with the conventional polyclonal antibodies against MBD1-4 are shown in the rightmost column for comparison.

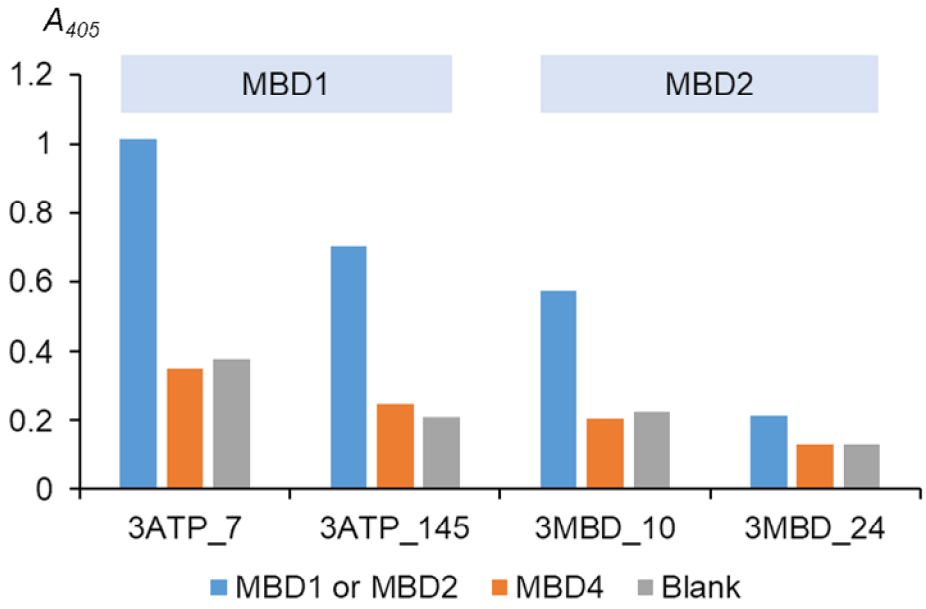

Fig. S2 Selection of Nanobodies against MBD1 and MBD2 by ELISA. The microplate wells were coated with either MBD1 or MBD2 (*blue*) as indicated above the graph, MBD4 (*orange*) as a negative control, or no antigen (blank, *grey*), and probed with crude periplasmic extracts from 190 *E. coli* colonies selected for further testing after two rounds of panning from the original library. Data for the Nanobodies chosen for further characterization is shown.

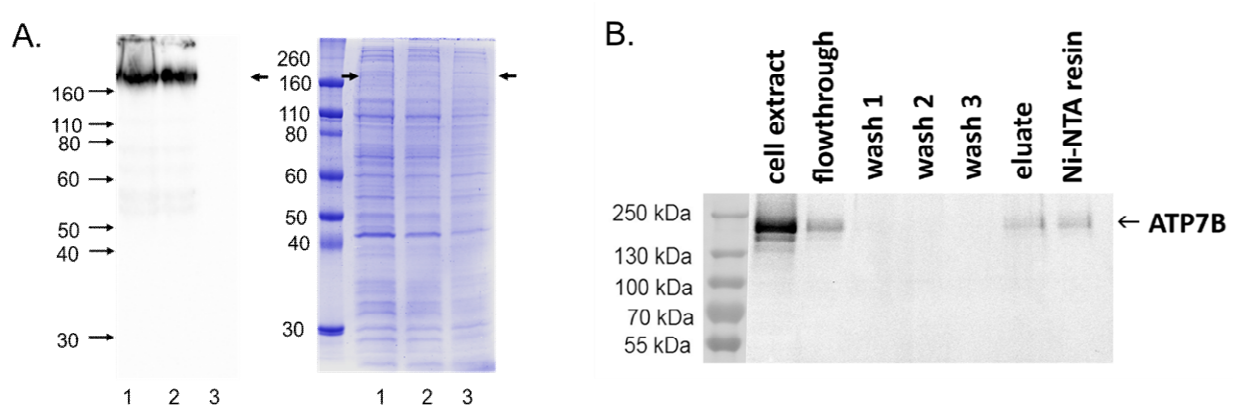

Fig S3. Pull-down of ATP7B from crude cell extract using the 5A51 Nanobody against MBD4.

A. The 5A51 Nanobody was tested by Western blot (*left panel, cf. Fig. S1*) of the HEK293 membranes expressing recombinant wild type ATP7B (*lane 1*), the D1027A mutant variant of ATP7B (*lane 2*), or endogenous ATP7B only (*lane 3*). The corresponding Coomassie stained gel is in the *right panel*. Positions of the molecular weight markers and their molecular weights in KDa are shown. Short arrows mark the position of ATP7B band.

B. Human fibroblasts mch46 overexpressing GFP-fusion of ATP7B were grown to ~80% confluency in the DMEM media supplemented with 10% FBS. Cells were washed twice with cold PBS and lysed in 50 mM HEPES, pH 7.4, 150 mM NaCl, 0.2% Triton X-100, containing protease inhibitor cocktail Ultra mini (Roche) and 1.5 mM PMSF on ice for 30 minutes, then centrifuged for 10 minutes at 6,000 x g. Supernatant was pre-cleaned with 10 µl of Ni-NTA resin for 20 minutes at 4°C and then incubated with 100 µg of 5A51 nanobodies for 30 minutes at 4°C. After incubation, 10 µl of Ni-NTA was added and incubated for 30 minutes at +4°C. The resin was washed 3 times with 500 µl of lysis buffer containing 5 mM imidazole. The protein was eluted with 25 µl of the lysis buffer supplemented with 250 mM imidazole. Samples were resolved on the 3.5-20% Laemmli gel, transferred onto nitrocellulose and incubated overnight at 4°C in 5% of GE Blocking reagent on PBST. Blots were incubated with rat anti-ATP7B antibodies (1:5,000 in 1% blocking reagent on PBST) for 1 hour at room temperature, washed 3 times for 5 minutes with 1% blocking reagent in PBST, then incubated with anti-rat secondary HRP-labeled antibodies (Santa Cruz, sc-2750) for 1 hour at room temperature, washed again, and ECL reaction was imaged using GBox (Syngene).

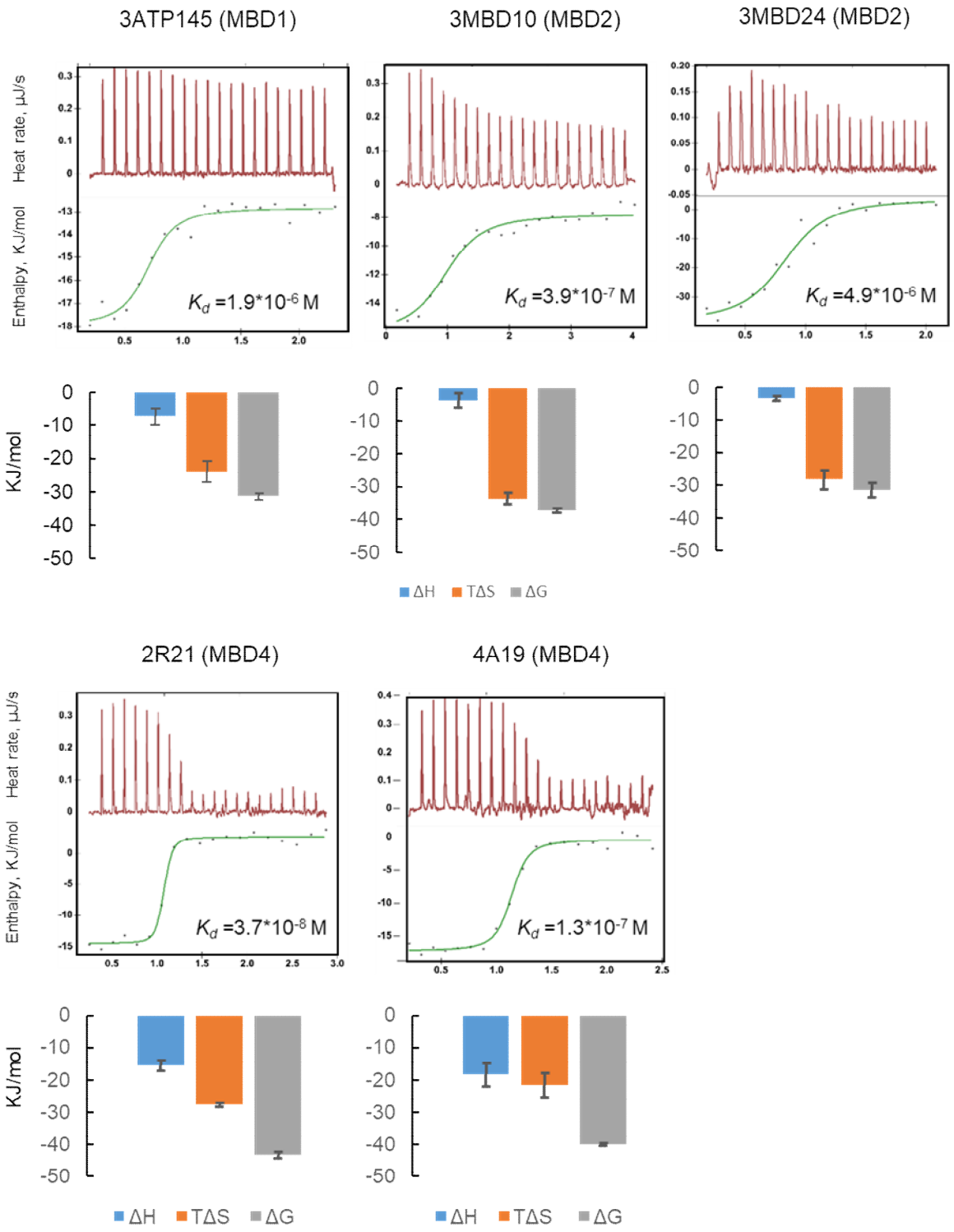

Fig. S4 Thermodynamic parameters of Nanobody binding to MBD1-4. (A) Thermograms and dissociation constants of various Nanobodies for binding to *apo*-MBD1-4. **(B)** Enthalpic and entropic contributions to the free energy change of Nanobody binding.